CRYSTAL GROWTH & DESIGN

ARTICLE

pubs.acs.org/crystal

In Vitro Synthesis of High Mg Calcite under Ambient Conditions and Its Implication for Biomineralization Process

Xia Long, Yurong Ma,* and Limin Qi*

Beijing National Laboratory for Molecular Sciences (BNLMS), State Key Laboratory for Structural Chemistry of Unstable and Stable Species, College of Chemistry, Peking University, Beijing 100871, P.R. China

Supporting Information

ABSTRACT: Instead of calcite or aragonite, thermodynamically unstable magnesium-bearing calcite occurs in many marine organisms such as sea urchin, sea star, corallina algae, and so on. However, the formation process of biogenic high-magnesium calcite has been an enigma. In this work, high-magnesium calcite in pure phase was synthesized in large yield via polymer-stabilized amorphous calcium magnesium carbonate (ACMC) precursors under mild conditions for the first time. The magnesium contents in Mg-bearing calcite can be exquisitely tuned from 15 to 40 mol % by changing the Mg/Ca ratio in mother solutions. We found appropriate polymer concentration windows for the synthesis of pure phase high Mg-calcite under defined crystallization conditions. It is proposed that the role of dextran sulfate sodium salt was to restrain the formation of aragonite, and the main role of poly(acrylic acid) was to stabilize ACMC. In this work, we designed a strategy to prepare thermodynamically unstable high Mg-calcite; that is, the preparation of polymer-stabilized precursor phase and the crystallization process were separated into two steps. This strategy might be extended to the synthesis of other thermodynamically unstable phases. The in vitro fabrication of pure high-magnesium calcite may give some indirect clues to the formation mechanism of biogenic Mg-calcite.

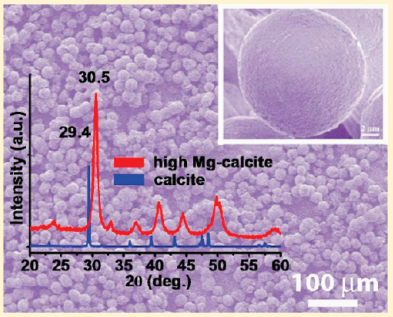

1. INTRODUCTION

Calcium carbonate is one of the most abundant biominerals in living organisms.[1−6] Compared with synthesized calcium carbonate, biogenic calcium carbonates often have special functions such as excellent mechanical[7] and optical properties[8] attributed to their unique chemical compositions, crystallographic orientations and hierarchical morphologies. The polymorphs of calcium carbonate include calcite, aragonite, vaterite, monohydracalcite, and hexahydrate calcium carbonate. Biogenic calcite with very high Mg content (20−45 mol %) has been found in many marine organisms such as echinoids sea urchins,[9,10] sea stars,[11] coralline algaes,[12] Alcyonarian corals,[13] and foraminifera,[13] even though Mg calcite containing more than 10 mol % Mg is thermodynamically unstable.[14] This thermodynamically metastable Mg calcite with Mg content higher than 10 mol % can be synthesized under very high temperature and high pressure.[15] The molar ratio of Ca to Mg is about 1:5 in the seawater, thermodynamically favorable for aragonite, but not Mg-bearing calcite.[16] Therefore, the formation of thermodynamically unstable high Mg calcite in marine organisms has been an enigma for a long time. Magnesium plays a role in stabilizing amorphous calcium mineral phase[17−20] and improving mechanical properties of biogenic Mg calcite.[21] Therefore, studying the formation mechanism of high Mg calcite not only has great importance in fundamental research of biomineralization but can also shed light on the design and fabrication of new functional materials.

In order to better understand the formation mechanism of high Mg calcite, many research groups have carried out in vitro syntheses of Mg calcite under mild conditions in their laboratories. Crystallization experiments using artificial or real seawater produced calcite with magnesium content less than 22 mol % along with other carbonate phases.[22−24] Using polysaccharides extracted from calcareous algae as additives, some researchers effectively diminished the inhibition of calcite growth in the presence of magnesium; however, no high magnesium calcite was formed in this system.[25,26] Raz et al. synthesized magnesium calcite particles with 34 mol % of magnesium along with aragonite in the presence of macromolecules extracted from skeletons of coralline algae.[17] By using molecules containing carboxylate groups[27−29] or alcohols[30] that usually occur in biomineral organisms as additives in solutions, calcite with up to 15 mol % magnesium content and aragonite were produced. Cheng et al. produced high magnesium-bearing calcite films via a polymer-induced liquid precursor process, which contained up to 26 mol % magnesium, but with low crystallization degree.[31] Other than preparation in solution, Aizenberg et al.[32] found that Mg^{2+} ions contributed to oriented nucleation of Mg-bearing calcite crystals with uniform nucleation plane, size, and morphology on self-assembled monolayers, and energy dispersive X-ray spectroscopy (EDS) showed the Mg content of up to 40 mol %. However, no further characterizations such as X-ray diffraction (XRD) were done to determine whether the obtained samples

Received: January 10, 2011
Revised: April 4, 2011
Published: May 05, 2011

were in a pure polymorph of Mg-bearing calcite or not.[32] Compared with biogenic high magnesium-bearing calcite, these synthesized Mg-bearing calcite products often contain a considerable amount of aragonite,[17,22,23,27,30,33] as well as a lot of amorphous calcium carbonate.[31]

Many studies indicate that macromolecules can stabilize amorphous precursors and control the crystallization process by adsorption to particular crystal surfaces,[34] step edges, or terraces.[35,36] Recently, it was found that carboxylated molecules can increase the Mg content in Mg-bearing calcite by up to 3 mol %[28] and promote the formation of Mg-enriched amorphous calcium carbonate.[29] Herein, we present a bioinspired approach to generate high Mg calcite with controlled magnesium content from 15 to 40 mol % via polymer-stabilized amorphous precursors under ambient conditions. It is worthy to note that under suitable polymer concentrations the high Mg calcite with high crystallinity may be obtained as the only polymorph in the product in large yield under mild temperature and pressure conditions for the first time. The Mg content in the as-synthesized Mg-bearing calcite is up to 40 mol %, very close to the Mg content (43.5 mol %) in sea urchin teeth,[9] so-called protodolomite, the highest found in biogenic minerals. It is found that the as-made high Mg calcite has a higher elastic modulus than pure calcite particles with similar size and morphology.

2. EXPERIMENTAL SECTION

Preparation of Intermediate Powder Precursor. Typically, a precursor suspension was prepared by quickly mixing 6 mL of Na_2CO_3 solution (0.5 M) with 9 mL of solution containing both $MgCl_2$ and $CaCl_2$ (Mg/Ca = 0, 0.5, 1, 2, 3, 4) in the presence of 6 mg of poly (acrylic acid, sodium salt, PAA) (M.W. = 5100, Aldrich) and 30 mg of dextran sulfate sodium salt (DexS) at 4 °C. A cloudy suspension formed immediately, indicating the formation of colloidal particles in the solution. The freshly prepared suspension was quickly filtered under a vacuum, and then washed with double distilled water and alcohol in sequence. The obtained powder precursor was later used for crystallization or characterization by XRD, Fourier transform IR spectroscopy, scanning electron microscopy (SEM), and transmission electron microscopy (TEM).

Controlled Transformation of Powder Precursor to High Mg Calcite. The prepared powder precursors were placed in a temperature and humidity controlled chamber (BPS-100CA, Shanghai, China) set to desired temperature and humidity for 1 to 4 days. The final products were dried in a drying oven under a vacuum at room temperature.

Characterizations. The morphologies of the obtained samples were determined using Hitachi FE-S4800 microscopy (SEM) at an accelerating voltage of 2.0 kV, JEOL JEM-200CX microscopy (TEM) at 160 kV, high resolution TEM (FETTECNAI F30) and polarized optical microscopy (Nikon ECLIPSE E600).

The final products were characterized in detail with an X-ray diffractometer (Rigaku Dmax-2000), Fourier transform infrared spectrometer (VECTOR22), energy dispersive X-ray detector (FETTECNAI F30), inductively coupled plasma-atomic emission spectrometer (PROFILE SPEC, Leeman) and thermal gravimetric analyzer (Q50 Thermogravimetric Analysis).

N_2 adsorption−desorption isotherms were determined on a Micromeritics ASAP-2010 apparatus. Prior to the measurement, the samples were heated at 200 °C for 3 h to remove water residues completely.

Thermal gravimetric analysis (TGA) was carried out on a TGA-Q50 (Thermal Analysis, U.S.A.) with the carrier gas of air at a heating rate of 10 °C/min.

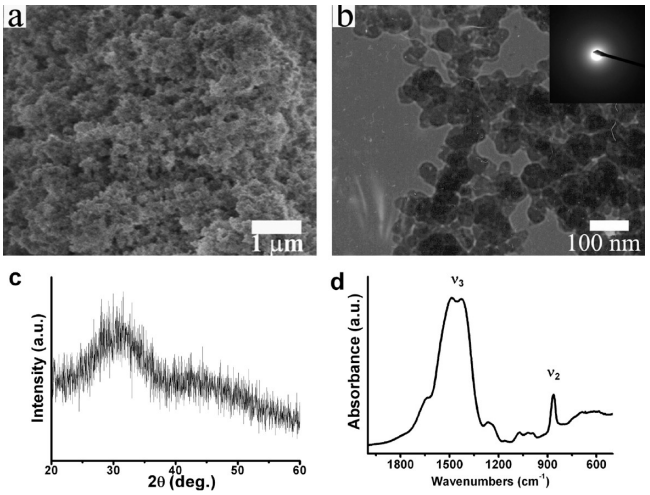

Figure 1. SEM image (a), TEM image (b) and ED pattern (b inset), XRD pattern (c), and FTIR spectrum (d) of amorphous calcium magnesium carbonate precursor obtained with Mg/Ca = 2, $[Ca^{2+}]$ = 0.17 M, [PAA] = 0.67mg/mL, [DexS] = 6.67 mg/mL

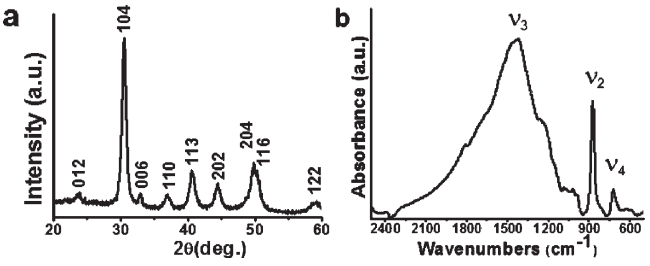

Figure 2. XRD pattern (a) and FTIR spectrum (b) of high Mg calcite formed after crystallizing at 80 °C, 70% RH for 4 days. The Mg/Ca ratio in the mother solution is equal to 2, $[Ca^{2+}]$ = 0.17 M. The concentrations of PAA and DexS in the mother solution are 0.67 mg/mL and 3.33 mg/mL, respectively.

Mechanical Testing of Magnesium-Bearing Calcite. High Mg-bearing calcite powders were embedded in epoxy resin (Buehler) at room temperature. Subsequently, they were lightly ground using 320#, 400#, 600#, 1000#, 2000# SiC paper and then polished by using 0.05 μm alumina suspension to form to a very smooth surface for indentation. Polished surfaces of Mg-bearing calcite were analyzed using a nanoindenter (TriboIndenter, Hysitron), equipped with Berkovich diamond tip. Mean modulus and hardness values were obtained from more than 10 load-depth curves for each sample at a depth of 100 nm.

3. RESULTS

Amorphous calcium magnesium carbonate (ACMC) precursor (Figure 1) was first prepared by mixing aqueous solutions of Na_2CO_3, $CaCl_2$, and $MgCl_2$ in the presence of poly(acrylic acid) sodium salt (PAA, MW 5100) (0.67 mg/mL) and dextran sulfate sodium salt (DexS) (3.33 mg/mL) quickly at 4 °C and separated from the mother solution by vacuum-assisted filtering. The SEM image in Figure 1a exhibited the intermediate powder composed of nanoparticles with diameters of about 10−20 nm. The TEM image and electron diffraction (ED) pattern in Figure 1b show that the nanoparticles are in the amorphous phase, which was further confirmed by XRD patterns and Fourier transfer infrared spectra (FTIR) in Figure 1c,d. After incubating ACMC powders

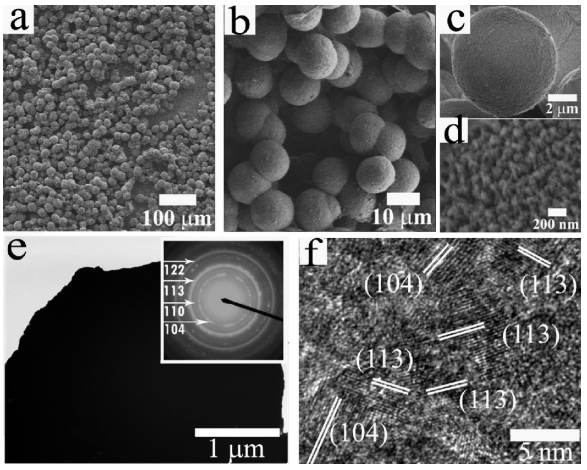

Figure 3. SEM (a−d), TEM (e), and HRTEM (f) images of high Mg calcite formed after crystallizing at 80 °C, 70% RH for 4 days. The Mg/Ca ratio in the mother solution is equal to 2, $[Ca^{2+}] = 0.17$ M. The concentrations of PAA and DexS in the mother solution were 0.67 mg/mL and 3.33 mg/mL, respectively. (a, b) Low magnification SEM images of Mg calcite microspheres; (c) high magnification SEM image of a microsphere in (a); (d) zoomed-in surface morphology of a microsphere in (c); (e) TEM image of a microsphere and electron diffraction pattern (inset) on a small area at the circumference of the microsphere; (f) HRTEM image of Mg-calcite microsphere.

in the chamber for four days under 80 °C and 70% relative humidity (RH), the obtained samples were dried in a desiccator overnight under a vacuum and then characterized by XRD, FTIR, and electron microscopies (Figures 2 and 3). The XRD pattern indicates that the obtained sample is well crystallized Mg-bearing calcite without any other polymorphs of calcium carbonate (Figure 2a). The 2θ of (104) peak shifts from 29.4° for pure synthetic calcite[37] to 30.5° in Figure 2a, with lattice spacing of 2.93 Å, and all the other peaks shift more or less to higher 2θ too. According to Goldsmith,[15] the crystal cell a_0 and c_0 of calcite decreases with the increase of Mg content in $Ca(Mg)CO_3$. The Mg content in the obtained Mg-bearing calcite is calculated to be about 39 mol % according to Goldsmith,[15] very close to the Mg content in polycrystalline matrix (43.5 mol %) of sea urchin teeth.[9] The magnesium content in the Mg-containing calcite presented here is significantly higher than ever reported in the literature[22−24,27,29−31] and much higher than that in thermodynamically stable Mg calcite (10 mol %).[14]

The FTIR spectrum in Figure 2b further proves the existence of well crystallized high Mg-bearing calcite without any other polymorphs. The absorption band of out-of-plane bending of carbonate, ν_4, appears at 726 cm^{-1} instead of 714 cm^{-1} for calcite, indicating the presence of high Mg content in calcite.[38] The ν_2 absorption band appeared at 875 cm^{-1}, typical for calcite. Moreover, the peak height ratios of ν_2 to ν_4 is 4.0, higher than the value of pure synthetic calcite ($\nu_2/\nu_4 = 3.0$),[39] also indicating its high crystallinity degree.

The magnesium content of the high Mg calcite characterized by inductively coupled plasma (ICP) and energy dispersive X-ray (EDX) analysis were 40 and 44 mol % (±3 mol %), respectively, fairly close to the XRD result (39 mol %). XRD shows the content of magnesium occluded in the crystal lattice of calcite, while ICP shows the average magnesium content in the final product, including both Mg calcite and ACMC. The Mg contents in the synthesized Mg calcite samples calculated by XRD and ICP were very close, probably due to their high crystallinity. In the following work, the Mg content in the product is calculated according to XRD data unless otherwise specified. Thermal gravimetric analysis (TGA) results (Figure S1, Supporting Information) indicate that the polymer content in the final Mg calcite is ~15 wt %, probably attached to the surface of the nanoparticles, subunits of microspheres. The large surface area of Mg-bearing calcite from N_2 adsorption−desorption isotherms (52.1 m^2/g) supports the above statement. In comparison, calcite microcrystals without magnesium synthesized under similar conditions has a much lower surface area (5.4 m^2/g).

The typical SEM images in Figure 3a−d indicate that high Mg calcite products are spherical particles with diameters of about 10 ± 3 μm, comprising nanoparticles on the surface. The electron diffraction (ED) pattern of one microsphere (Figure 3e inset) shows clear diffraction rings with d spacings of 2.92, 2.38, 2.14, and 1.51 Å, corresponding to d spacings of (104), (110), (113), and (122) of calcite, respectively, consistent with the d spacing values obtained from XRD pattern (Figure 2a). The high-resolution transmission electron microscopy (HRTEM) image (Figure 3f) displays lattice spacings of 2.93 and 2.17 Å, corresponding to (104) and (113) planes of calcite, respectively. Polarized optical microscopy (POM) images (Figure S2, Supporting Information) also show well-crystallized microspheres with birefringence. The above results indicate that the obtained high Mg calcite crystals are well crystallized microspheres composed of nanoparticles, with relatively uniform size in pure calicte polymorph.

To better understand the formation mechanisms of the high Mg calcite, reaction conditions such as crystallization time, temperature, humidity, ratio of Mg to Ca, and concentrations of polymer additives were also investigated. First, calcium carbonate samples were characterized after different crystallization times. Calcium carbonate precursor is composed of amorphous nanoparticles with diameters less than 100 nm (Figure S2, Supporting Information). After the precursor was kept under 80 °C, 70% RH for one day, only nanoparticles existed (Figure S3a,b, Supporting Information). However, after 2 days, some quasi-spherical particles appeared, coexisting with nanoparticles (Figure S3c,d, Supporting Information). More quasi-spherical particles formed after elongating the crystallization time from 2 to 3 days (Figure S3c−f, Supporting Information). It is deduced from the above results that the ACMC nanoparticles work as the intermediate precursor for the formation of high Mg calcite microspheres, which is a very popular transformation process for the biogenic calcite minerals.[39−43]

Mg calcite samples were prepared at various Mg/Ca ratios with the other experimental conditions similar to that in Figure 2. The XRD patterns in Figure 4a show that the obtained samples are mainly composed of Mg calcite, mixed with a very small amount of aragonite. With the increase of Mg/Ca ratios from 0 to 4, the 2θ value of calcite (104) planes in the XRD patterns shifted from 29.4° to 30.6° and the d spacing of (104) decreased from 3.04 Å to 2.92 Å (Figure 4a), because of the Mg^{2+} replacement of Ca^{2+} in calcite lattices. The ν_4 absorption band of Mg calcite shifts from 712 cm^{-1} to a higher wavenumber, 728 cm^{-1}, with the increase of Mg/Ca ratio from 0 to 3 (Figure 4b). The blue shift of ν_4 absorption band in the FTIR spectra is also due to the replacement of calcium cations by magnesium cations in calcite lattices.[15,31] The Mg content calculated from the (104) peak shift in the XRD spectra according to Goldsmith's work[15] increases from 15−20 mol % (Mg/Ca = 0.5) to 40 mol % (Mg/Ca = 3)

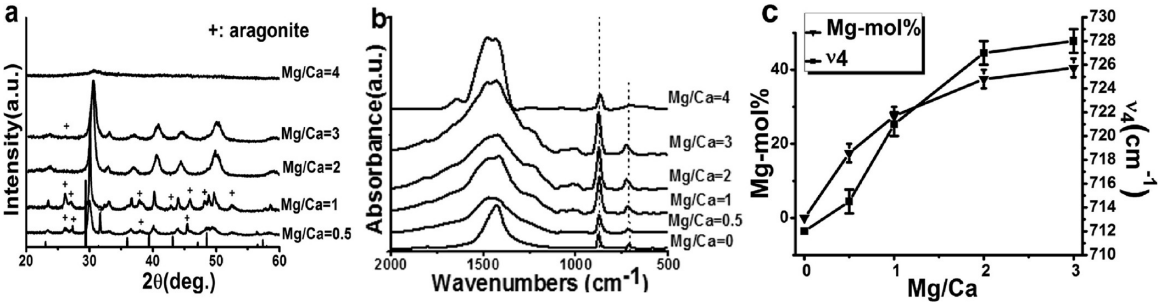

Figure 4. XRD patterns (a) and FTIR spectra (b) of Mg-bearing calcite formed from mother solution with varied Mg/Ca ratios, in the presence of 0.67 mg/mL PAA and 3.33 mg/mL DexS. The concentrations of $CaCl_2$ are 0.1 M, 0.125M, 0.17 M, 0.25 M, 0.33 M, and 0. 5M, when Mg/Ca = 4, 3, 2, 1, 0.5 and 0, respectively. Temperature and humidity are 80 °C and 70% RH, and the crystallization time is 4 days. (c) Relation curves of Mg mol % calculated from (104) *d* spacings in the XRD patterns and ν_4 absorption band position from FTIR spectra with different Mg/Ca ratios.

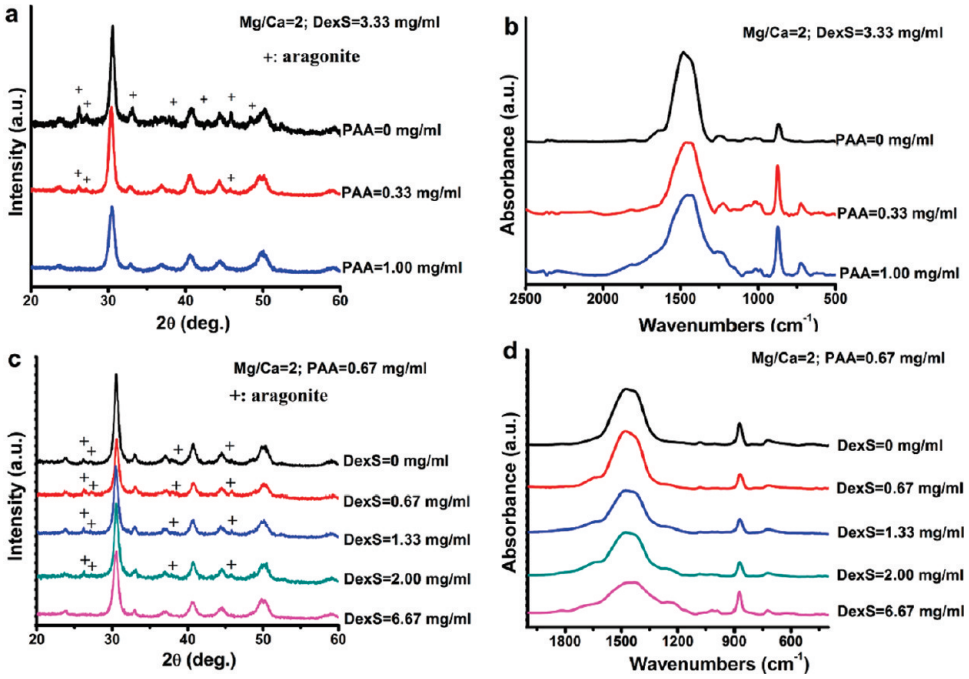

Figure 5. XRD patterns (a, c) and FTIR spectra (b, d) of high Mg calcite formed with Mg/Ca = 2, $[Ca^{2+}]$ = 0.17 M, by using various amounts of additives. The crystallization conditions were 80 °C, 70% RH and the crystallization time is four days. (a, b) [PAA] = 0.33 mg/ml, and various concentrations of DexS; (c, d) [DexS] = 3.33 mg/mL and various concentrations of PAA; XRD pattern (c) and FTIR spectrum (d) of Mg calcite formed with Mg/Ca = 2, [PAA] = 0.67 mg/mL and various concentrations of DexS. The crystallization conditions were 80 °C, 70% RH and the crystallization time is four days.

with increasing Mg/Ca ratio (Figure 4c). When the Mg/Ca ratio was increased to 4, ν_2 appeared at 867 cm^{-1} while the ν_4 peak disappeared, indicating the final product is amorphous,[44,45] consistent with the corresponding XRD pattern in Figure 4a. The very high stability of amorphous phase at an Mg/Ca ratio of 4 further proves the important role of Mg ions for stabilizing amorphous phase both in vivo and in vitro.[18−20,46−48] The above XRD and FTIR results are further summarized in detail in Table S1, Supporting Information. The intensity ratios of ν_2/ν_4 shown in Table S1, Supporting Information range from 3.5 to 5.5 (except Mg/Ca = 4), revealing relatively high crystallinity of the obtained Mg-bearing calcite. It is obvious from the above results that the Mg/Ca ratio in the mother solution has a very strong influence on Mg content in the crystallized Mg calcite. The higher Mg/Ca ratio, the higher the Mg content in the final product. The above conclusion is consistent with Stanley's work related to the Mg content in the coralline algae.[12] However, when the Mg/Ca ratio was fixed, the change of the polymer concentration had no effect on Mg content in Mg-bearing calcite (Figures 5 and S4).

The addition of additives has a strong influence on the polymorph of calcium carbonate in both biogenic minerals[49,50] and synthetic[4,51] systems. Herein, different concentrations of PAA and DexS were used for the synthesis of Mg-bearing calcite under fixed crystallization temperatures, humidities, and Mg/Ca ratios (Figures 5, 6, and S4). Our goal in this work is to synthesize well crystallized high Mg calcite in single polymorph. Thus, the colors in Figure 6 only highlight the existence of the polymorphs while ignoring the contents of different polymorphs, even though the main peak intensity ratios from XRD patterns are in the 0.02−0.15 range for aragonite and calcite, or in the 0.02−0.39

dx.doi.org/10.1021/cg200028x |*Cryst. Growth Des.* 2011, 11, 2866–2873

range for monohydrocalcite and calcite. One can see clearly from the XRD patterns in Figures 5 and S4 that the main peak intensities of aragonite and monohydrocalcite are mostly very low, about 2−7% of that of Mg-bearing calcite by calculation, except for the situations when the concentration of PAA was zero (Figures 5a and S4a). Thus, it is reasonable to claim that the contents of aragonite or monohydrocalcite in these samples are both very low.

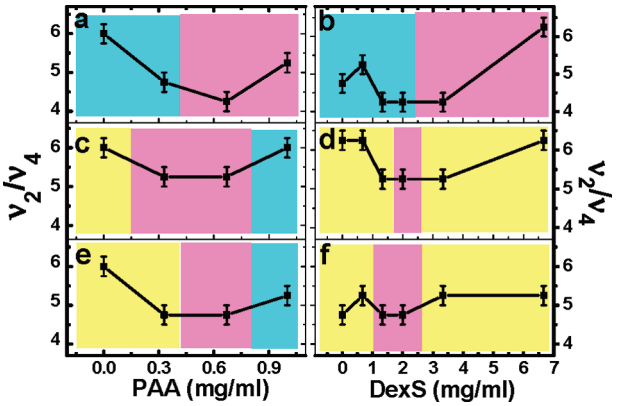

Figure 6. The crystallization degrees and polymorphs of Mg-bearing calcium carbonate synthesized by using different concentrations of additives. The higher ν_2/ν_4 ratios of Mg-bearing calcite in the FTIR spectra, the lower crystallization degrees of Mg calcite. The polymorphs of Mg-bearing calcium carbonate are represented by different colors. Pure phase Mg-calcite, Mg-calcite mixed with a small amount of aragonite, and Mg-calcite mixed with a small amount of monohydrocalcite are presented in pink, light blue, and yellow, respectively. (a, b) Mg/Ca = 2, crystallization temperature and humidity: 80 °C and 70% RH; (c, d) Mg/Ca = 1, crystallization temperature and humidity: 50 °C and 70% RH; (e, f) Mg/Ca = 1, crystallization temperature and humidity: 50 °C and 60% RH; (a) DexS = 3.33 mg/mL; (b) PAA = 0.67 mg/mL; (c) DexS = 2 mg/mL; (d) PAA = 0.67 mg/mL; (e) DexS = 1.33 mg/mL; (f) PAA = 0.67 mg/mL. The concentrations of calcium ions are 0.17 M and 0.25 M when Mg/Ca ratios are 2 and 1, respectively. And the crystallization time is 4 days for all the samples.

Figures 5 and 6a,b summarized the XRD and FTIR results of the samples obtained at 80 °C and 70% RH and the Mg/Ca ratio in the mother solution is equal to 2. Mg calcite is the main phase, coexisting with a small amount of aragonite at low concentrations of PAA (0−0.33 mg/mL) and DexS (0−2.00 mg/mL). High Mg calcite in single polymorph can be obtained at appropriate concentration windows for PAA (0.67−1.00 mg/mL) and for DexS (3.33−6.67 mg/mL). And the ν_2/ν_4 ratio of these samples increased from 4.0 to 6.0 with the increase of polymer concentrations, indicating a decrease of their crystallinity degree.

The influence of polymer concentration was further investigated with the Mg/Ca ratio at 1 and crystallization conditions at 50 °C and 70% RH (Figure 6c,d). Pure phase high Mg calcite was obtained when the concentrations of PAA and DexS were 0.33−0.67 mg/mL and 1.33 mg/mL, respectively. Other polymer concentrations led to the formation of mixed polymorphs of Mg calcite and a small amount of monohydrocalcite or aragonite (Figure 6c,d). At a lower humidity setting, 60% RH, the optimum polymer concentrations for pure phase high Mg calcite are a bit different, given as c(PAA) = 0.67 mg/mL, c(DexS) = 1.33−2.00 mg/mL (Figures 6e,f and S4). At fixed DexS concentration, low PAA concentrations (0−0.33 mg/mL) led to impurity from monohydrocalcite, and higher PAA concentrations induced impurity from aragonite (Figure 6c,e). When the PAA concentration was kept at 0.67 mg/mL, both higher and lower DexS concentrations (0−0.67 mg/mL, 3.33 mg/mL) led to impurity

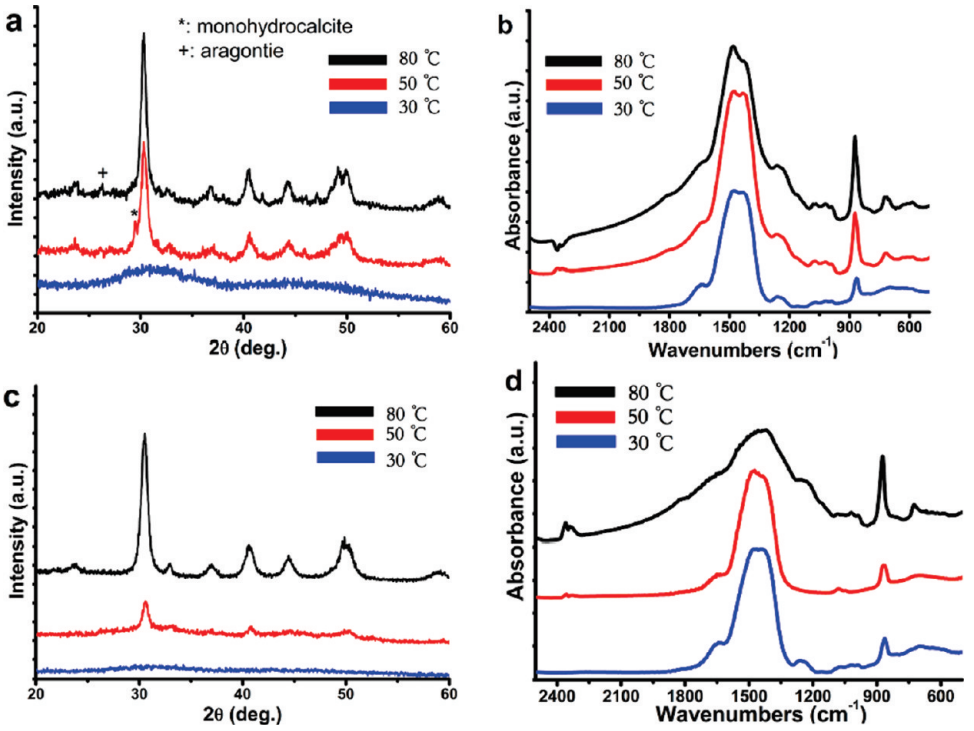

Figure 7. XRD (a, c) and FTIR (b, d) spectra of Mg-bearing calcite crystallized at different temperatures and humidities. (a, b) Mg/Ca = 1; (c, d) Mg/Ca = 2; [PAA] = 0.67 mg/mL; [DexS] = 3.33 mg/mL; humidity was 70% RH; the crystallization time is 4 days. The concentration of calcium ions are 0.17 M and 0.25 M when Mg/Ca ratios are 2 and 1, respectively.

dx.doi.org/10.1021/cg200028x |*Cryst. Growth Des.* 2011, 11, 2866–2873

Table 1. Mechanical Properties of Mg-Bearing Calcite with Different Magnesium Contents Characterized by Nanoindentation[a]

	Mg/Ca	Mg mol %	Er (Gpa)[a]	SD for Er	*H* (Gpa)	SD for *H*
calcite (Iceland spar)[b]		0	96.5 (n = 16)	2.2	4.0	0.1
dolomite (cleavage)[b]		50	112.3 (n = 16)	5.2	6.9	0.8
calcite microcrystals	0	0	35.9 (n = 13)	7.2	3.2	0.4
Mg-calcite 1	0.5	15−20	44.5 (n = 43)	4.7	3.1	0.6
Mg-calcite 2	1	25−30	46.1 (n = 19)	3.7	3.1	0.4
Mg-calcite 3	2	35−40	45.6 (n = 18)	4.5	3.0	0.4

[a] Er: elastic modules; *H*: hardness; SD: standard deviation; n: number of indentations. The Er and *H* values are obtained from indentations within 100 nm. [b] Both the single crystalline calcite (Iceland Spar) and the dolomite (cleavage) were bought from Ward's Natural Science.

from monohydrocalcite (Figure 6d,f). Under any given crystallization conditions, we can always find optimum concentration windows for the synthesis of well crystallized high Mg calcite in pure phase.

The crystallization temperature and humidity are very critical factors for the crystallization degree of Mg-bearing calcite (Figure 7). In general, the higher Mg/Ca ratio, the higher temperature is needed for good crystallization degree. It can be seen from Figure 7 that 50 and 80 °C are needed when the Mg/Ca ratio is equal to 1 and 2, respectively. Magnesium has the ability to stabilize ACMC.[19] Therefore, it is more difficult to crystallize the amorphous phase with higher Mg^{2+} concentration in the reaction system. On the other hand, the higher temperature, the easier to crystallize calcium carbonate. Thus, it is deduced that at a higher Mg/Ca ratio, higher temperature is required for the preparation of well crystallized Mg-bearing calcite.

The elastic modulus (Er) and hardness (H) of high Mg calcite microspheres were characterized by nanoindentation. The Mg-bearing calcite samples were embedded into resin and then polished before nanoindentation (Figure S5a, Supporting Information). Some microspheres were broken during polishing and we only measured the microsphere cross sections with smooth surfaces. No cracks emanating along the corners of the indentations were seen (Figure S5b, Supporting Information), indicating the high fracture toughness of the Mg calcite microspheres.[21] Table 1 shows some of the most informative mechanical parameters of Mg calcite with different magnesium contents. It could be seen from the table that high Mg calcite samples (Mg-calcite 1, 2, and 3) have higher Er values than Mg-free calcite microcrystals synthesized under similar conditions except that there are no Mg ions in the mother solution (Table 1 and Figure S5b, Supporting Information). However, the hardness values of these four samples are very similar, about 3 GPa. The existence of polymers and Mg ions probably contributes to the higher modulus of high Mg calcite, like the reinforcement mechanism of Mg and biomolecules in biogenic high Mg calcite.[21] However, it remains unclear by now why only the modulus of the Mg calcite is higher than that of calcite microcrystals, but not the hardness. The relation between the mechanical properties and Mg and polymer contents in the Mg calcite is still under investigation. All these three samples have lower hardness and modulus than that of single crystalline geological calcite (Iceland Spar) and dolomite (cleavage) with a size in centimeters, probably due to the porous feature of the Mg-containing calcite mcirospheres.

4. DISCUSSION

De Yoreo and his collaborators pointed out that the formation of Mg-rich carbonates is probably through nonclassical processes from transient amorphous phase,[29] similar to many other in vivo and in vitro systems.[4,18,52] In this work, we realized the synthesis of high Mg calcite with controlled Mg content from 15 to 40 mol % under ambient conditions according to nonclassical crystallization strategies from polymer-stabilized ACMC.

Experimental conditions such as the Mg/Ca ratios in the mother solutions, crystallization temperature, relative humidity, and concentrations of PAA and DexS are all critical for the formation of high Mg calcite in pure polymorph. First, the Mg/Ca ratio in the mother solution has a very strong influence on the Mg content in the crystallized Mg calcite. The higher the Mg/Ca ratio, the higher the Mg content in the final product. Second, the higher the Mg/Ca ratio used, the higher the crystallization temperature necessary for reasonable crystallization degree, consistent with the stability role of Mg ion on ACC.[18,19,46,48] Third, we can always find optimum windows of the polymer concentrations for the synthesis of high Mg calcite at a defined crystallization temperature, humidity, and Mg/Ca ratio. The optimum concentration windows of additives are 0.67−1.00 mg/mL for PAA and 3.33−6.67 mg/mL for DexS for the synthesis of pure phase high Mg calcite with Mg content 36−39 mol %, with an Mg/Ca ratio of 2 and crystallization under 80 °C and 70% RH. It is proposed that the role of DexS is mainly to restrain the formation of aragonite[26] and also to remove the hydration shell of Mg ions by its −OH groups, in the end to induce the formation of Mg bearing calcite. The main role of PAA is supposedly to stabilize ACMC, similar to its role to stabilize amorphous calcium carbonate (ACC) in many systems.[53] When PAA concentration increases from 0 to 0.33 mg/mL, the crystallization degree increases, probably because a small amount of PAA can induce the crystallization of ACC in the presence of magnesium.[19]

A lower minimum concentration of DexS, ranging from 1.33 mg/mL to 2.00 mg/mL, is necessary for the synthesis of pure phase high Mg calcite, when ACMC is crystallized at a relatively low temperature of 50 °C and Mg/Ca ratio equal to 1. At low temperature and inappropriate polymer concentrations, one should not ignore the existence of another polymorph byproduct, monohydrocalcite, even though its percentage in the final product is very low. The stoichiometric formula for monohydracalcite ($CaCO_3 \cdot H_2O$) is the same as that of hydrated ACC in the spicules of *Pyura pachydermatina*.[54] Monohydrocalcite usually forms in the environment with high magnesium content[55] and has a solubility higher than calcite, aragonite, and vaterite. Thus, monohydrocalcite easily transforms into calcite or aragonite at higher temperature.[54] Probably this is why monohydracalcite only exists in the final product obtained at 50 °C but not at 80 °C. The main mineral in the calcareous corpuscles of *Mesocestoides corti* is monohydrocalcite,[56] unusually found in biominerals, but probably an intermediate phase in the biogenic mineralization

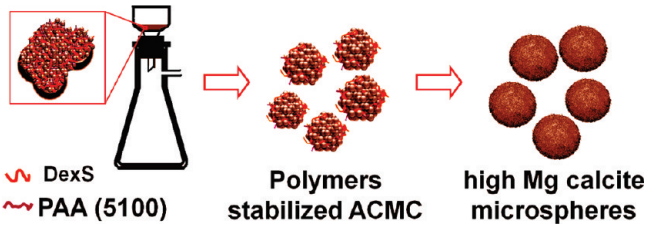

Figure 8. Schematic of the formation process of high Mg-bearing calcite via polymer-stabilized amorphous calcium magnesium carbonate (ACMC).

process, like stable hydrated ACC and transient anhydrous ACC.[18]

It is well-known that ACC is unstable and will readily transform into calcium carbonate crystals in ambient conditions in the absence of any additives.[48,57] Even via control of polymers like polycarboxylate or biomolecules from coralline algae, a mixture of Mg calcite with aragonite was obtained via crystallization in aqueous solution.[17] It can be seen from our results that it turns out to be much easier to control the formation of high Mg calcite as the only polymorph, like in many biogenic high Mg calcite systems,[9,11−13] if we separate the preparation of ACMC precursor and the crystallization process in the solid state by the control of polymers into two steps. The formation mechanism of high Mg calcite is proposed as follows (Figure 8). First, it is essential to obtain the ACMC precursor by separating it from the mother solution by vacuum filtering and washing with alcohol because the amorphous phase is very unstable in aqueous solution. Second, appropriate temperature and relative humidity, which have a great influence on crystallization kinetics of Mg-calcite, were used to control the transformation rate of PAA-stabilized ACMC to magnesium-bearing calcite in a few days. If the crystallization rate is too fast, the polymorphs will not be controlled very well and other polymorphs such as aragonite or monohydrocalcite might form. If the crystallization is too slow, the final product might include a lot of amorphous phase or have low crystallization degree after four days of crystallization. Our aim in this work is to get high Mg calcite in pure phase with high crystallization degree after a reasonable period of time. The concentrations of PAA and DexS need to be exquisitely controlled for the preparation of high Mg calcite in pure phase under given crystallization temperature, humidity, and Mg/Ca ratios.

The naturally occurring biological organisms learn how to form what they need under ambient conditions after evolving for millions of years, for example, very high Mg calcite nanocomposites with fantastic mechanical properties in sea urchin teeth.[21] Bioinspired fabrication of high Mg-calcite in pure phase in this work is based on balancing the effects of additives, which stabilize ACMC and inhibit the formation of aragonite, and the influence of temperature and humidity, which play an important role in the crystallization kinetics of ACMC. However, biological organisms can effectively control the mineralization process by using macromolecules such as polyaspartic acid and polysaccharides under mild conditions.[26,50]

It is worthy to note that both the PAA and DexS are commercially available and the yield of the high Mg calcite can be very high, more than 5 g in one beaker in our experiments, and there is no hindrance at all for scaling up if necessary. This means that this simple methodology for high Mg calcite synthesis could be applied in the industries directly. Mg-bearing calcite particles with better mechanical properties will meet potential applications in the fields such as paper, paint, coating, etc.

5. CONCLUSIONS

In conclusion, well-crystallized high Mg calcite with controlled Mg content was synthesized as the only polymorph by the controlled transformation from polymer-stabilized ACMC precursor via nonclassical crystallization process under optimized temperature and relative humidity. To the best of our knowledge, this is the first report on the synthesis of high Mg calcite in pure phase and high yield with controlled magnesium content from 15 to 40 mol % under ambient conditions. The success of our approach relies on two key points: the collaborative effect of optimum amounts of PAA and DexS, which stabilized amorphous precursors and inhibit the formation of aragonite, and appropriate temperature and humidity for controlled crystallization rate from ACMC to high Mg calcite. The formation mechanism might be similar to that of biogenic high Mg calcite. Moreover, nanoindentation tests indicate that high Mg calcite has a higher Young's modulus than calcite without Mg synthesized under similar conditions. The formation of high Mg calcite in large yield in such a simple way may find potential application in industry.

■ ASSOCIATED CONTENT

Ⓢ Supporting Information. TGA curve, polarized optical microscopy images, SEM images, FTIR and XRD spectra, table of characteristic absorption bands in FTIR and diffraction peaks in XRD of calcite. This material is available free of charge via the Internet at http://pubs.acs.org.

■ AUTHOR INFORMATION

Corresponding Author

*E-mail: yurong.ma@pku.edu.cn (Y.M.); liminqi@pku.edu.cn (L.Q.).

■ ACKNOWLEDGMENT

We thank Ming Qiang for her help during nanoindentation experiments. This work was supported by National Basic Research Program of China (Grants 2007CB815602 and 2007CB936201) and NSFC (Grants 50902002, 20873002, 21073005, and 50821061).

■ REFERENCES

(1) Lowenstam, H. A.; Weiner, S. *On Biomineralization*; Oxford University Press: New York, 1989.

(2) Mann, S. *Biomineralization, Principles and Concepts in Bioinorganic Materials Chemistry*; Oxford University Press: Oxford, 2001.

(3) Gower, L. B. *Chem. Rev.* **2008**, *108*, 4551–4627.

(4) Meldrum, F. C.; Cölfen, H. *Chem. Rev.* **2008**, *108*, 4332–4432.

(5) Cusack, M.; Freer, A. *Chem. Rev.* **2008**, *108*, 4433–4454.

(6) Bäuerlein, E. *Handbook of Biomineralization: Biological Aspects and Structure Formation*, 1st ed.; Wiley-VCH: New York, 2009; Vol 1, p 472.

(7) Mayer, G. *Science* **2005**, *310*, 1144–1147.

(8) Aizenberg, J.; Tkachenko, A.; Weiner, S.; Addadi, L.; Hendler., G. *Nature* **2001**, *412*, 819–822.

(9) Schroeder, J. H.; Dwornik, E. J.; Papike, J. J. *Geol. Soc. Am. Bull.* **1969**, *80*, 1613–1616.

(10) Ma, Y. R.; Aichmayer, B.; Paris, O.; Fratzl, P.; Meibom, A.; Metzler, R. A.; Politi, Y.; Addadi, L.; Gilbert, P. U. P. A.; Weiner, S. *Proc. Natl. Acad. Sci. U. S. A.* **2009**, *106*, 6048–6053.
(11) Gayathri, S.; Lakshminarayanan, R.; Weaver, J. C.; Morse, D. E.; Kini, R. M.; Valiyaveettil, S. *Chem.—Eur. J.* **2007**, *13*, 3262–3268.
(12) Stanley, S. M.; Ries, J. B.; Hardie, L. A. *Proc. Natl. Acad. Sci. U. S. A.* **2002**, *99*, 15323–15326.
(13) Chave, K. E. *J. Geol.* **1954**, *62*, 266–283.
(14) Chave, K. E.; Deffeyes, K. S.; Weil, P. K.; Garrels, R. M.; Thompson, M. E. *Science* **1962**, *157*, 33–34.
(15) Goldsmith, J. R.; Graf, D. L.; Heard, H. C. *Am. Mineral.* **1961**, *46*, 453–457.
(16) Kitano, Y.; Hood, D. W. *J. Oceanogr. Soc. Jpn.* **1962**, *18*, 141–145.
(17) Raz, S.; Weiner, S.; Addadi, L. *Adv. Mater.* **2000**, *12*, 38–42.
(18) Addadi, L.; Raz, S.; Weiner, S. *Adv. Mater.* **2003**, *15*, 959–970.
(19) Tao, J. H.; Zhou, D. M.; Zhang, Z. S.; Xu, X. R.; Tang, R. K. *Proc. Natl. Acad. Sci. U. S. A.* **2009**, *106*, 22096–22101.
(20) Politi, Y.; Batchelor, D. R.; Zaslansky, P.; Chmelka, B. F.; Weaver, J. C.; Sagi, I.; Weiner, S.; Addadi, L. *Chem. Mater.* **2010**, *22*, 161–166.
(21) Ma, Y.; Cohen, S. R.; Addadi, L.; Weiner, S. *Adv. Mater.* **2008**, *20*, 1555–1559, *12*, 952–956.
(22) Glover, E. D.; Sippel, R. F. *Geochim. Cosmochim. Ac.* **1967**, *31*, 603.
(23) Devery, D. M.; Ehlmann, A. J. *Am. Mineral.* **1981**, *66*, 592–595.
(24) Towe, K. M.; Malone, P. G. *Nature* **1970**, *226*, 348–349.
(25) Kitano, Y.; Hood, D. W. *Geochim. Cosmochim. Ac.* **1965**, *29*, 29–41.
(26) Wada, N.; Okazaki, M.; Tachikawa, S. *J. Cryst. Growth* **1993**, *132*, 115–121.
(27) Wada, N.; Yamashita, K.; Umegaki, T. *J. Colloid Interface Sci.* **1999**, *212*, 357–364.
(28) Stephenson, A. E.; DeYoreo, J. J.; Wu, L.; Wu, K. J.; Hoyer, J.; Dove, P. M. *Science* **2008**, *322*, 724–727.
(29) Wang, D. B.; Wallace, A. F.; De Yoreo, J. J.; Dove, P. M. *Proc. Natl. Acad. Sci. U. S. A.* **2009**, *106*, 21511–21516.
(30) Falini, G.; Gazzano, M.; Ripamonti, A. *Chem. Commun.* **1996**, 1037–1038.
(31) Cheng, X. G.; Varona, P. L.; Olszta, M. J.; Gower, L. B. *J. Cryst. Growth* **2007**, *307*, 395–404.
(32) Han, Y. J.; Aizenberg, J. *J. Am. Chem. Soc.* **2003**, *125*, 4032–4033.
(33) Jiang, J.; Gao, M.-R.; Qiu, Y.-H.; Wang, G.-S.; Liu, L.; Cai, G.-B.; Yu, S.-H. *CrystEngComm* **2011**, *12*, 952–956.
(34) Addadi, L.; Weiner, S. *Proc. Natl. Acad. Sci. U. S. A.* **1985**, *82*, 4110–4114.
(35) De Yoreo, J. J.; Wierzbicki, A.; Dove, P. M. *CrystEngcomm* **2007**, *9*, 1144–1152.
(36) Teng, H. H.; Dove, P. M.; Orme, C. A.; De Yoreo, J. J. *Science* **1998**, *282*, 724–727.
(37) Maslen, E. N.; Streltsov, V. A.; Streltsova, N. R. *Acta. Crystallogr. B* **1993**, *49*, 636–641.
(38) Dauphin, Y. *Appl. Spectrosc.* **1999**, *53*, 184–190.
(39) Politi, Y.; Arad, T.; Klein, E.; Weiner, S.; Addadi, L. *Science* **2004**, *306*, 1161–1164.
(40) Nassif, N.; Pinna, N.; Gehrke, N.; Antonietti, M.; Jager, C.; Colfen, H. *Proc. Natl. Acad. Sci. U. S. A.* **2005**, *102*, 12653–12655.
(41) Aizenberg, J.; Muller, D. A.; Grazul, J. L.; Hamann, D. R. *Science* **2003**, *299*, 1205–1208.
(42) Gebauer, D.; Volkel, A.; Colfen, H. *Science* **2008**, *322*, 1819–1822.
(43) Mahamid, J.; Sharir, A.; Addadi, L.; Weiner, S. *Proc. Natl. Acad. Sci. U. S. A.* **2008**, *105*, 12748–12753.
(44) Aizenberg, J.; Lambert, G.; Addadi, L.; Weiner, S. *Adv. Mater.* **1996**, *8*, 222–226.
(45) Beniash, E.; Aizenberg, J.; Addadi, L.; Weiner, S. *Proc. Natl. Acad. Sci. U. S. A.* **1997**, *264*, 461–465.
(46) Loste, E.; Wilson, R. M.; Seshadri, R.; Meldrum, F. C. *J. Cryst. Growth* **2003**, *254*, 206–218.
(47) Davis, K. J.; Dove, P. M.; De Yoreo, J. J. *Science* **2000**, *290*, 1134–1137.
(48) Raz, S.; Hamilton, P. C.; Wilt, F. H.; Weiner, S.; Addadi, L. *Adv. Funct. Mater.* **2003**, *13*, 480–486.
(49) Weiner, S.; Levi-Kalisman, Y.; Raz, S.; Addadi, L. *Connect. Tissue. Res.* **2003**, *44*, 214–218.
(50) Gotliv, B. A.; Addadi, L.; Weiner, S. *ChemBiochem* **2003**, *4*, 522–529.
(51) Sommerdijk, N. A. J. M.; de With, G. *Chem. Rev.* **2008**, *108*, 4499–4550.
(52) Gower, L. B. *Chem. Rev.* **2008**, *108*, 4551–4627.
(53) Jiang, F. G.; Yang, Y. H.; Huang, L.; Chen, X.; Shao, Z. Z. *J. Appl. Polym. Sci.* **2009**, *114*, 3686–3692.
(54) Neumann, M.; Epple, M. *Eur. J. Inorg. Chem.* **2007**, 1953–1957.
(55) Tlili, M. M.; Ben Amor, M.; Gabrielli, C.; Joiret, S.; Maurin, G.; Rousseau, P. *J. Raman Spectrosc.* **2002**, *33*, 10–16.
(56) Senorale-Pose, M.; Chalar, C.; Dauphin, Y.; Massard, P.; Pradel, P.; Marin, M. *Exp. Parasitol.* **2008**, *118*, 54–58.
(57) Faatz, M.; Grohn, F.; Wegner, G. *Adv. Mater.* **2004**, *16*, 996–1000.